# REVISITING 2D ANALYSIS OF BRIDGING IN ADHESIVELY BONDED DCB SPECIMENS

*Youliang Guan[1], Bo Chen[1,3], Romesh C. Batra[1], Donatus C. Ohanehi[1], John G. Dillard[2], David A. Dillard[1*]*

*[1] Department of Engineering Science and Mechanics, [2] Department of Chemistry,*

*[3] Currently at the Dow Chemical Company, Piscataway, NJ 08854.*

*Virginia Polytechnic Institute and State University, Blacksburg, Virginia, 24061*

## Introduction

When adhesive bonds are separated beyond their capacity, in some situations, the failure may occur along one interface for some distance, and then switch to the other one, leaving in the wake an adhesive bridge suspended between the two adherends. This phenomenon is commonly encountered when testing DCB specimens displaying interfacial failures with an adhesive which has sufficient extensibility to bridge the crack without failure. Failure to properly account for the bridge would increase the apparent fracture energy if this occurred in a bond being tested. The analysis presented herein will extend the analysis presented in [1], recognizing that although such bridging phenomenon are infrequent in well bonded structural bonding, it can be quite common in demolding processes where molded parts, often quite fragile, must be removed from adherends consisting of the two mold halves. Other area of considerable interest has been in the bridging of cracks by one phase in multiphase materials.

In practice, this bridge may often be relatively uniform across the width of the specimen, permitting a 2D analysis as is presented herein. The analysis treats the suspended adhesive bridge as a membrane, assuming that the flexural rigidity is small because of the small thickness of the bridge compared to other dimensions in the model. This membrane is assumed to be linear elastic, as are the two adherends. As shown in Figure 1 (b), the adhesive bridge exerts equal tractions on the upper and lower adherends. Based on these assumptions, the strain energy release rates (SERRs) at the three resulting crack tips are calculated and discussed. The analysis predicts the sequences of debonding events for several bridge configurations. Interactions of the cracks are also discussed based on the three SERR curves.

## Analysis

When a DCB specimen is loaded, the crack may propagate along one interface for some distance, and then a second crack may initiate along the opposite interface. Continued loading will result in both cracks propagating, leaving behind a suspended adhesive bridge which may exist at a relatively shallow angle with respect to the adherends. The bridge results in three debond tips located at crack lengths of $a_1$, $a_2$, and $a_3$, as shown in Figure 1.

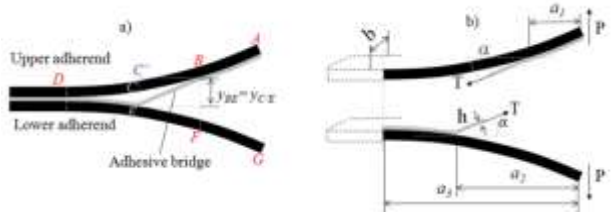


Figure 1. Model of the adhesive bridging problem with geometric parameters, external loads, and tractions exerted by the bridge: a) Schematic of the 2D model; b) Cantilever beam models for the two adherends and definitions of three crack lengths.

The adherends are assumed to be identical, resulting in a 2D DCB specimen that, except for the bridge, appears to be symmetric and globally loaded in mode I. The adherends, as well as the bond, are assumed to have width $b$. The thickness of the adhesive layer and bridge is $h$. Ignoring deflections within the bonded adhesive layer, the adherends can be considered to be cantilever beams fixed at crack tip 3. Based on simple beam theory, the differential equations can be solved using appropriate boundary conditions at points A, B, D, E, and G. (Point E is not shown in the Fig.)

Using a coordinate system with the origin at point D, the derivation can be started from the shear force equation in the Euler-Bernoulli beam theory, $EI\frac{d^3y}{dx^3}=V(x)$. The solutions of the deflections can be shown with three components: contribution from external load $P$, from shear force $T\sin\alpha$, and from moment exerted by $T\cos\alpha$.

Since the traction $T$ is an internal force, external work performed on the specimen enters solely through the displacement of load P, which can be considered to be applied by an Instron machine with one adherend fixed and the other one moving. A quasi-static loading condition is considered in this model, where the external forces are assumed to remain constant. Therefore, based on the definition, the SERR is the energy dissipated during fracture per unit of newly created fracture surface area. For each crack in this model, it is equal to the difference in the external work and strain energy for each step of crack increment.

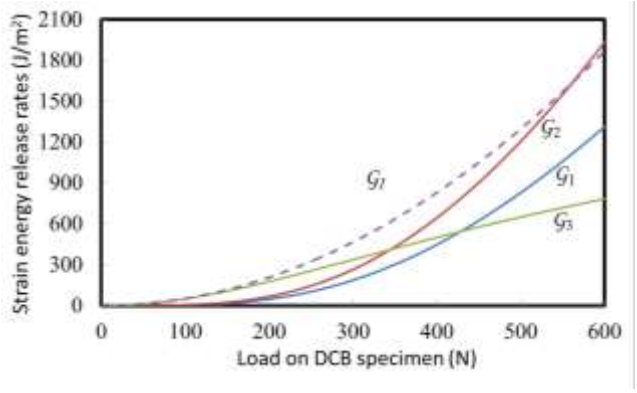


Figure 2. SERR curves for the three crack tips as functions of load $P$, with $a_1 = 50mm$, $a_2 = 68mm$, $a_3 = 200mm$ (Assumes no crack propagation, adhesive with modulus of $3GPa$, thickness of $0.25mm$, bond width of $25.4mm$, aluminum adherends with modulus of $70GPa$, width of $25.4mm$, and thickness of $12.7mm$).

Obviously, as shown in Figure 2, the three SERR curves are different from each other, so that, when $P$ is assumed, the values of $\mathcal{G}_1$, $\mathcal{G}_2$, and $\mathcal{G}_3$ are usually different. The curve for the SERR for a specimen without bridging ($\mathcal{G}_I$), is also shown. Results calculated from other crack length configurations show similar trends if the cracks are assumed to be stationary: $\mathcal{G}_2$ is always higher than $\mathcal{G}_1$; $\mathcal{G}_3$ will be higher than $\mathcal{G}_2$ at the beginning but becomes lower after a certain value of $P$.

Also, this model is useful to predict the crack propagation sequence. One such propagation sequence for a DCB specimen with aluminum adherends is shown in Figure 3, with assumed fracture energy $\mathcal{G}_c = 300J/m^2$ along the bonded surfaces. Assume that $a_2 = 51mm$ at the beginning, and debonding from crack tip 1 to crack tip 3 develops on the upper adherend due to some weakness at this interface. Therefore, it is reasonable to assume $a_1 = 50mm$ and $a_3 = 52mm$ as representative values. In these calculations, the increment of crack lengths in each step is assumed to be $0.1mm$. When the crosshead displacement increases, $\mathcal{G}_3$ increases quickly to $\mathcal{G}_c$ and thus $a_3$ increases first. After $a_3$ reaches a critical length, $\mathcal{G}_3$ will be a little lower than $\mathcal{G}_2$. Therefore, $\mathcal{G}_2$ will be the next to reach $\mathcal{G}_c$. Thus, $a_2$ increases instead of $a_3$. Thus, with the $\mathcal{G}_c$ value set up as the goal, the competition between $\mathcal{G}_2$ and $\mathcal{G}_3$ will drive the propagation of crack 2 and crack 3. Since the value of $\mathcal{G}_1$ is always less than $\mathcal{G}_2$, crack $a_1$ will never propagate under the conditions analyzed here. In reality, if $\mathcal{G}_c$ is a constant, crack 2 and crack 3 will be growing continuously, but at different rates. Since the numerical increment is very small, it is a reasonable simulation for the continuous crack propagation.

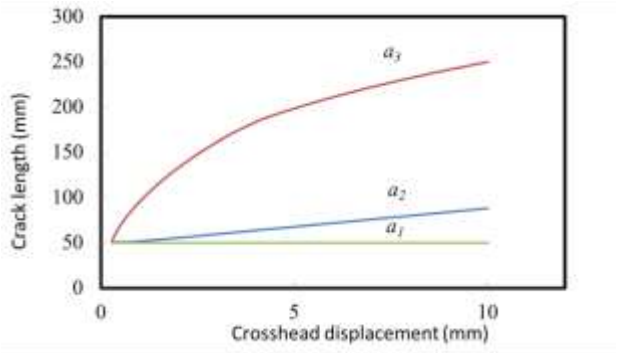


Figure 3. Crack propagation sequences calculated by the 2D model. (The initial crack lengths, $a_1 = 50mm$, $a_2 = 51mm$, and $a_3 = 52mm$ are assumed. Fracture energy is assumed to be $\mathcal{G}_c = 300J/m^2$ along the bonded surfaces. The increment in calculation is assumed to be $0.1mm$ for all the three crack lengths.)

As previously shown in Figure 2, there is always an intersection, and "balance point", between the $\mathcal{G}_2$ and $\mathcal{G}_3$ curves regardless of the assumed crack lengths. Therefore, it is useful to investigate the similarity in these curves. This balance point can give us the critical value of P or the SERR where the competition between $\mathcal{G}_2$ and $\mathcal{G}_3$ comes to a draw.

Therefore, it is useful to analyze the balance points by altering key factors (such as crack lengths or material properties). If we assume that the bridge will not break or yield, the balance points can be calculated by solving equations and then be connected continuously. For example, in Figure 4, if there is no propagation in crack 1 and crack 2 but let $a_3$ increase from $75mm$ to $85mm$, a series of balance points can be plotted. Note that this

figure is not a simulation of real crack propagation, but only an example to show the trends of balance points. Therefore, the similarity of SERR curves can be linked and described by the balance points. When altering the key factors, the shapes of the three SERR curves are similar but the graphs are "zoomed in" or "zoomed out."

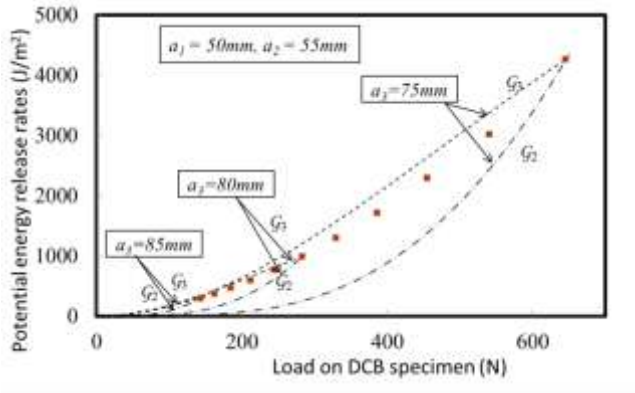


Figure 4. Balance points with different values of $a_3$ ( $a_1 = 50mm$ and $a_2 = 55mm$ are fixed).

The other similarity can be found if the crack propagation sequences with various initial crack length configurations are plotted. Therefore, regardless of the geometry and material properties, if a constant $G_c$ is assumed, when the specimen is loaded up, both $G_2$ and $G_3$ will be approaching $G_c$. One of them will get there first and that crack will propagate for certain distance until there comes a balance point. Physically, beyond this value, both cracks will propagate simultaneously. This point of view can also provide useful predictions to the crack propagation sequences.

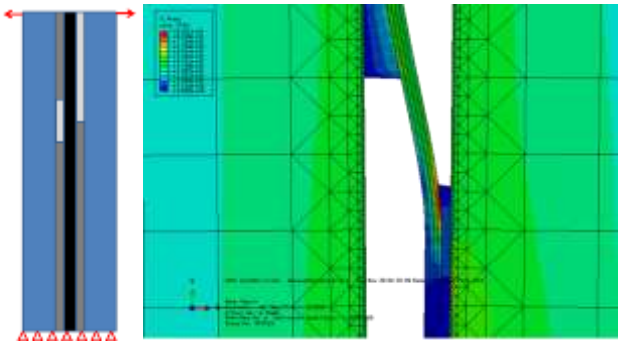

Figure 5. Schematic of geometry, loads, boundary conditions, and result of stress distribution from the simulation of the 2D bridging problem in ABAQUS (The thickness of interfaces shown is only for visualization, and is very small in the calculation).

Simulations of bridging DCB specimen test were also performed with the commercial finite element software ABAQUS™, with the same geometry as that used in Figure 2, and the same initiate crack lengths in the analysis with the beam theory. Cohesive elements were applied in this model and the Cohesive Zone Method (CZM) is applied as material property for the two interfaces and the same fracture energy value is assigned. The propagation sequences are simulated by the software. The difference between the present analysis with the beam theory and the ABAQUS is very small.

## Conclusions

In summary, the bridging problem has been studied by using a 2D DCB specimen model. Based on Euler-Bernoulli beam theory and linear elastic material behavior, the deflections, strains, and SERRs have been calculated for adhesively bonded aluminum/epoxy system. The effects of bridging on the loads and crosshead displacements of a DCB specimen are studied. Compared with a non-bridging DCB specimen (with the same crosshead displacement or crack length $a = a_3$), the load P is higher for the bridging models. Therefore, fracture energy recorded in mode I test of DCB specimen will be overestimated if the bridging effect is not accounted for.

Similarities in the SERR curves can be found. By investigating the balance points where the crack propagation priority is switched, the crack propagation sequence can be predicted when the fracture energy is assumed for the interfaces. There is also a relationship between the interaction of cracks $a_2$ and $a_3$. Once material properties are assumed, cracks $a_2$ and $a_3$ will propagate by following a fixed law. Therefore, in summary, these investigations can be useful for the understanding and prediction of the behavior of bridging DCB specimens (or demolding processes). These results can also provide useful information to develop strategies to control the crack propagation.

## Acknowledgements

The authors are grateful for support from the National Science Foundation (NSF/CMMI Award No. 0826143).

## References

1. D. A. Dillard and B. Chen, "A 2-D Analysis of Bridging in Adhesively Bonded DCB Specimens," in *Proceedings of the 1997 SEM Spring Conference*,, 1997, pp. 236-237.